Journal of Biological Methods | **2022** | **Vol**. 9(1) | e159
DOI: 10.14440/jbm.2022.381

PROTOCOL

Site-specific nanobody-oligonucleotide conjugation for super-resolution imaging

Laura Teodori[1,2‡], Marjan Omer[1,2‡], Anders Märcher[1,3], Mads K. Skaanning[1,3], Veronica L. Andersen[1,3], Jesper S. Nielsen[1,2], Emil Oldenburg[1,2], Yuchen Lin[1], Kurt V. Gothelf[1,3,4], Jørgen Kjems[1,2,3*]

[1]Interdisciplinary Nanoscience Center (iNANO), Aarhus University, Gustav Wieds Vej 14, 8000 Aarhus C, Denmark
[2]Center for Cellular Signal Patterns (CellPAT), Aarhus University, Gustav Wieds Vej 14, 8000 Aarhus C, Denmark
[3]Center for Multifunctional Biomolecular Drug Design (CEMBID, Aarhus University, Gustav Wieds Vej 14, 8000 Aarhus C, Denmark
[4]Department of Chemistry, Aarhus University, Gustav Wieds Vej 14, 8000 Aarhus C, Denmark

‡These authors contributed equally to this work.

*Correspondence author: Jørgen Kjems, Email: jk@mbg.au.dk

Competing interests: The authors have declared that no competing interests exist.

Abbreviations used: AMP, ampicillin; BLI, bio-layer interferometry; BSA, bovine serum albumin; h, hour; HER2, human epidermal growth factor 2 receptor; IPTG, isopropyl β-D-1-thiogalactopyranoside; MWCO, molecular weight cut-off; O/N, overnight; PAGE, polyacrylamide gel electrophoresis; PAINT, points accumulation for imaging in nanoscale topography; PALM, photoactivated localization microscopy; pAzF, 4-azido-*L*-phenylalanine; SMLM, single-molecule localization microscopy; SPAAC, strain-promoted azide-alkyne cycloaddition; SPEC, spectinomycin; STORM, stochastic optical reconstruction microscopy; VCAM1, vascular cell adhesion molecule-1; UAA, unnatural amino acid

Received September 7, 2021; Revision received December 17, 2021; Accepted December 24, 2021; Published March 1, 2022

ABSTRACT

Camelid single-domain antibody fragments, also called nanobodies, constitute a class of binders that are small in size (~15 kDa) and possess antigen-binding properties similar to their antibody counterparts. Facile production of recombinant nanobodies in several microorganisms has made this class of binders attractive within the field of molecular imaging. Particularly, their use in super-resolution microscopy has improved the spatial resolution of molecular targets due to a smaller linkage error. In single-molecule localization microscopy techniques, the effective spatial resolution can be further enhanced by site-specific fluorescent labeling of nanobodies owing to a more homogeneous protein-to-fluorophore stoichiometry, reduced background staining and a known distance between dye and epitope. Here, we present a protocol for site-specific bioconjugation of DNA oligonucleotides to three distinct nanobodies expressed with an N- or C-terminal unnatural amino acid, 4-azido-*L*-phenylalanine (pAzF). Using copper-free click chemistry, the nanobody-oligonucleotide conjugation reactions were efficient and yielded highly pure bioconjugates. Target binding was retained in the bioconjugates, as demonstrated by bio-layer interferometry binding assays and the super-resolution microscopy technique, DNA points accumulation for imaging in nanoscale topography (PAINT). This method for site-specific protein-oligonucleotide conjugation can be further extended for applications within drug delivery and molecular targeting where site-specificity and stoichiometric control are required.

Keywords: bioconjugation, click chemistry, site-specificity, nanobodies, super-resolution microscopy

BACKGROUND

Nanobodies are single-domain antibody fragments (V_HHs) derived from camelids, which retain the structural and functional properties of naturally occurring heavy chain-only antibodies. Therefore, nanobodies are smaller [1] (12–15 kDa, ~2.5 × 4 nm) than traditional IgG antibodies (150 kDa, ~14.2 × 8.5 nm) but still bind target antigens with similar affinity and specificity [2,3]. Moreover, nanobodies can be produced in yeast and bacteria, which opens up a number of engineering options that are not always available for monoclonal antibodies.

Because of their small size, nanobodies are particularly well suited for single-molecule localization microscopy (SMLM) [4], also known as "nanoscopy", which includes a group of super-resolution techniques that predict with high precision and accuracy the spatial coordinates of a single fluorescent molecule. For visualization of subcellular structures, SMLM variations, such as photoactivated localization microscopy (PALM) [5,6], stochastic optical reconstruction microscopy (STORM) [7], direct STORM (dSTORM) [8] and DNA points accumulation for imaging in nanoscale topography (PAINT) [9] routinely utilize two separate antibodies. These are a primary antibody to ensure target specificity, and a secondary antibody coupled to either multiple synthetic fluorescent dyes, as in dSTORM, or DNA oligonucleotides as in DNA-PAINT *via N*-hydroxysuccinimidyl (NHS) esters to ε-amines on lysine residues. However, aside from a lack of site-specificity and

How to cite this article: Teodori L, Omer M, Märcher A, Skaanning MK, Andersen VL, Nielsen JS, Oldenburg E, Lin Y, Gothelf KV, Kjems J. Site-specific nanobody-oligonucleotide conjugation for super-resolution imaging. *J Biol Methods* 2022;9(1):e159. DOI: 10.14440/jbm.2022.381

stoichiometric control, this widely used coupling strategy creates a linkage error of ~10–20 nm due to the distance between dyes or DNA strand and the protein of interest (POI), which has been reported to give high background staining [10]. Combined with the use of large IgG antibodies, this fluorescence labeling strategy has been found to cause uncertainty in the localization precision of the POI, as the actual position of imaging signal would be separated by > 20 nm.

To circumvent a large linkage error, and thereby improve spatial accuracy for the target, the use of nanobodies raised against the POI is beneficial, owing to their small size and easy handling [11-13]. Unfortunately, current methods for direct attachment of fluorescent dyes or DNA oligonucleotides to nanobodies involve unspecific coupling *via* maleimide-thiol or amine-NHS reactions [14]. NHS reactions are specific for primary amines but most proteins, including nanobodies, contain more than one lysine which inevitably leads to heterogeneous labeling and potential interference with epitope binding. For site-specific labeling, the introduction of an engineered cysteine on the nanobody C-terminus has become a preferred strategy [10,15]. However, although maleimide reactions are specific for free thiols, the resulting thioether bond is subject to thiol exchange reactions which are particularly prevalent in serum and within cells. Site-specific coupling of nanobodies to oligonucleotides can also be achieved through Sortase A-mediated conjugation [16], although this approach requires an additional reaction and purification step, as well as the production of recombinant enzyme.

Here, we present a scalable method for the production of nanobodies carrying a single biorthogonal azide functional group and their subsequent one-step bioconjugation to a fluorophore and DNA oligonucleotide for super-resolution imaging. The azide is introduced using the method pioneered by Schultz and colleagues, in which an unnatural amino acid (UAA) is introduced *via* an ectopic aminoacyl transferase engineered to recognize the amber stop-codon UAG [17]. Importantly, the method for nanobody expression and conjugation presented here does not require specialized equipment and can be carried out in standard molecular biology laboratories.

We demonstrate the feasibility of the method by producing three distinct nanobodies, each with its own unique specificity. Two nanobodies, 2Rs15d and 2Rb17c, target the human epidermal growth factor receptor 2 (HER2) [18] while a third nanobody, cAbVCAM1-5, (for simplicity referred to as VCAM1-5) targets the vascular cell adhesion molecule-1 (VCAM1) receptor [19]. All three nanobodies were expressed in *E. coli* and purified using affinity chromatography. Subsequently, each nanobody was covalently conjugated to a DNA oligonucleotide or Cy5 fluorophore using copper-free click chemistry and purified by ion-exchange or size-exclusion chromatography. The resulting bioconjugates are > 95% pure and retain their affinity and specificity when studied by bio-layer interferometry (BLI) and DNA-PAINT super-resolution microscopy. This method presents a useful strategy to improve spatial resolution and to allow measurement of the absolute number of POIs by quantitative super-resolution microscopy like quantitative PAINT (qPAINT), owing to the stoichiometric control of the labeling strategy [20].

MATERIALS

Reagents

- ✓ 4-azido-*L*-phenylalanine (Chem-Impex, Cat. #06162)
- ✓ pUltra-CNF (Addgene, plasmid #48215)
- ✓ pMECS (kindly provided by Serge Muyldermans), (see Note 1)
- ✓ Novex™ TBE-Urea Gels, 15% (ThermoFisher, Cat. #EC-68852BOX)
- ✓ NuPAGE Bis-Tris gels, 4%–20% (ThermoFisher, Cat. #NP-0321BOX)
- ✓ Ampicillin (AMP) (Sigma Aldrich Cat. #A9518-25G) stock solution: 50 and 100 mg/ml, sterile-filtered
- ✓ Spectinomycin (SPEC) (Sigma Aldrich, Cat. #S4014-5G) stock solution: 50 and 100 mg/ml, sterile-filtered
- ✓ Isopropyl β-D-1-thiogalactopyranoside (IPTG) (BioChemica, Cat. #APA1008.0025) stock solution: 1 M, sterile-filtered
- ✓ Glycerol bidistilled 99.5% (VWR, Cat. #24388.295)
- ✓ Sodium chloride (VWR, Cat. #27810.295)
- ✓ Agar (VWR, Cat. #20767.232)
- ✓ Yeast extract, granulated (Fisher BioReagents, Cat. #BP9727-2)
- ✓ Tryptone, granulated (Fisher BioReagents, Cat. #BP9726-2)
- ✓ SOC media (Invitrogen Cat. #15544-034)
- ✓ Salt buffer: 0.17 M KH_2PO_4, 0.72 M K_2HPO_4, pH 7
- ✓ TES solution: 0.2 M TrisHCl, pH 8, 0.5 mM EDTA, 0.5 M sucrose
- ✓ Glucose 10% (w/v) solution, sterile-filtered
- ✓ Äkta binding buffer: 20 mM sodium phosphate pH 7.4, 500 mM NaCl, 20 mM imidazole
- ✓ Äkta elution buffer: 20 mM sodium phosphate pH 7.4, 500 mM NaCl, 500 mM imidazole
- ✓ Ion exchange binding buffer: 20 mM Tris, pH 8.0
- ✓ Ion exchange elution buffer: 20 mM Tris, pH 8.0, 500 mM NaCl
- ✓ HisTrap™ Fast Flow column, 5 ml (Cytiva, Cat #17524802)
- ✓ ENrich Q High-resolution anion exchange column (BioRad, Cat. # 7800001)
- ✓ Slide-A-Lyzer™ Dialysis Cassettes, 3.5 kDa cut-off (ThermoFisher, Cat. #66332)
- ✓ Amicon® Ultra-4 Centrifugal Filter Units (3 kDa cut-off, Cat. #UFC800324)
- ✓ Zeba Spin Desalting Columns, 7K MWCO (ThermoFisher, Cat. #89882)
- ✓ Protein A biosensors (Sartorious, Cat. #18-5010)
- ✓ DBCO-Cy5 (Sigma-Aldrich, Cat. #777374-1MG)
- ✓ DBCO-modified DNA oligonucleotides (docking strands) (Metabion):
- ✓ 7× R3d: 5′ - DBCO - CTC TCT CTC TCT CTC TCT C - 3′
- ✓ 5× R1d: 5′ - DBCO - TCC TCC TCC TCC TCC TCC T - 3′
- ✓ Cy3B-labeled DNA oligonucleotide (imager strand) (Metabion):
  - R1i: 5′ - AGG AGG A – Cy3B - 3′
- ✓ *E. coli* strain WK6
- ✓ 90 nm Standard Gold Nanoparticles, 0.1 mM in 1× PBS (Cytodiagnostics, Cat. #G-90-100)
- ✓ 40× PCA solution (Sigma-Aldrich, Cat. #37580-25G-F)
- ✓ 100× PCD solution (Sigma-Aldrich, Cat. #P8279-25UN)
- ✓ 100× Trolox solution (Sigma-Aldrich, Cat. #238813-1G)

NOTE: An alternative to the pMECs vector is the commercially available expression vector pET-22b(+) compatible with the BL21 *E. coli* strain. The nanobody sequence can be incorporated between the restriction sites NcoI and XhoI in the pET22b(+) vector and custom synthesized by GenScript.

Recipes

- ✓ Terrific broth (TB)
  - For 1 L media, prepare 24 g Yeast extract, 12 g Tryptone, 4.5 ml glycerol in a 5 L Erlenmeyer flask. Add demineralized water to 0.9 L, then autoclave using a program that reaches 121°C for 20 min.
  - Before use, supplement the flask with 100 ml salt buffer, 1 ml 2 M $MgCl_2$, 0.5 ml 100 mg/ml AMP, 0.5 ml 50 mg/ml SPEC and 10 ml 10% glucose solution.
- ✓ 2× TY
  - In a 2 L reagent flask, prepare 16 g Tryptone, 10 g Yeast extract, 5 g NaCl. Add 1 L demineralized water and autoclave.
- ✓ Luria-Bertani (LB) + agar
  - To prepare 1 L LB with agar, add 10 g Tryptone, 5 g Yeast extract, 10 g NaCl and 16 g Agar to a 2 L reagent flask. Fill up to 1 L with demineralized water and autoclave.
  - When the media has cooled down to 50–60°C, add the appropriate antibiotics, stir gently and use immediately for preparation of agar plates in Petri dishes.

NOTES: (1) All buffers are pH adjusted with either NaOH or HCl. All buffers used for bacterial protein expression and intended for use in chromatography should be passed through a 0.22 µm filter before use. Store buffers containing imidazole away from light and at 4°C for long-term storage. (2) The LB + agar media without antibiotics can be prepared and stored at 4°C for 1–2 months. When needed, the media can be heated in a microwave or water bath at 60°C.

Equipment

- ✓ Water bath or block heater
- ✓ Erlenmeyer flask, 5 L
- ✓ Horizontal rotator or equivalent
- ✓ Slide-A-Lyzer, 3.5K MWCO cut-off (ThermoFisher, Cat. #66332)
- ✓ UV spectrophotometer/Fluorometer (DeNovix DS-11) or equivalent
- ✓ ÄKTA Start Protein purification system (Cytiva) https://www.cytivalifesciences.com/en/us/shop/chromatography/chromatography-systems/akta-start-p-05773
- ✓ BioRad NGC Medium Pressure Chromatography System. https://www.bio-rad.com/en-dk/category/ngc-medium-pressure-liquid-chromatography-systems?ID=MFCV7415
- ✓ XCell SureLock Mini-Cell Electrophoresis System. https://www.thermofisher.com/dk/en/home/life-science/protein-biology/protein-gel-electrophoresis/protein-gel-electrophoresis-chamber-systems/xcell-surelock-mini-vertical-electrophoresis-system.html
- ✓ OctetRed96 System. https://www.sartorius.com/en/products/protein-analysis/octet-label-free-detection-systems/octet-red96e
- ✓ Oxford Nanoimager S (ONI) or any TIRF microscope: https://oni.bio/nanoimager/

PROCEDURES

Synthesis of 4-azido-*L*-phenylalanine

The UAA 4-azido-*L*-phenylalanine (pAzF) can be purchased from several manufacturers, such as Sigma Aldrich or Chem-Impex. The cost of pAzF is considerable for large-scale production of nanobodies but it can be produced in-lab in few steps from inexpensive commercially available starting materials. In this study, pAzF was synthesized in-house following the detailed protocol reported by Gregory A. Weiss and co-workers [21]. The method is scalable to at least 50 g starting material. In short, the procedure is as follows:

1. Prepare the potassium salt of the commercially available Boc-4-iodo-L-phenylalanine by washing Boc-4-iodo-L-phenylalanine with a separated mixture of 1:1 ethyl acetate and 0°C 4 M KOH (10 ml of each pr. gram starting material). Subsequent washings with ethyl acetate, collection of the organic phase and removal of volatiles *in vacuo* provides the potassium salt.
2. Resolubilize the formed potassium salt in thoroughly degassed 70% aq. EtOH (prepared by bubbling nitrogen or argon gas through the solution), use approximately 5 ml pr. gram of starting material. The solution is kept under argon or nitrogen gas. To the solution is then added sodium ascorbate (0.05 eq.), potassium hydroxide (0.05 eq.), sodium azide (2.0 eq.), *N,N'*-dimethylethylenediamine (3.3 eq.) and copper (I) iodide (0.2 eq.). The reaction is stirred for 18 h under an inert atmosphere.
3. Filter and remove volatiles *in vacuo*, then add ethyl acetate and 0°C 2 M KOH (10 ml of each pr. gram starting material). Shake the solution in a separatory funnel and perform an additional extraction with ethyl acetate. Wash the combined organic phase with 0°C 250 mM HCl in saturated NaCl (15 ml pr. gram starting material). Removal of volatiles *in vacuo* then provides *N*-Boc-4-azido-*L*-phenylalanine.
4. Remove the Boc protecting group with 1:1 2 M sulfuric acid and dioxane for 2 h, final concentration 200 mM. Remove approximately half of the solvent *in vacuo*, and carefully add 0°C 4 M KOH until a pH of 7 is reached. Collect the formed precipitate by filtration.

5. Heat the filtrate to boiling in a 1:1 EtOH:H_2O solution (30 ml/g starting material). Filter the mixture and discard the filtered solid. Then crystalize the product from the filtrate either by cooling or slow addition of hot EtOH and subsequent cooling.

Expression of pAzF-modified nanobodies in *E. coli*

The following section describes the procedure for bacterial expression of nanobodies with pAzF incorporated in either the N- or C-terminal end (**Fig. 1**). Competent WK6 *E. coli* cells are transformed with the suppressor plasmid (pUltra) and the expression plasmid (pMECS), encoding the nanobody sequence with an N-terminal pelB leader sequence, a C-terminal hexahistidine tag (6× His), and an amber stop codon (TAG) positioned either immediately after the pelB leader sequence (N-terminal UAA), or before the 6× His tag (C-terminal UAA).

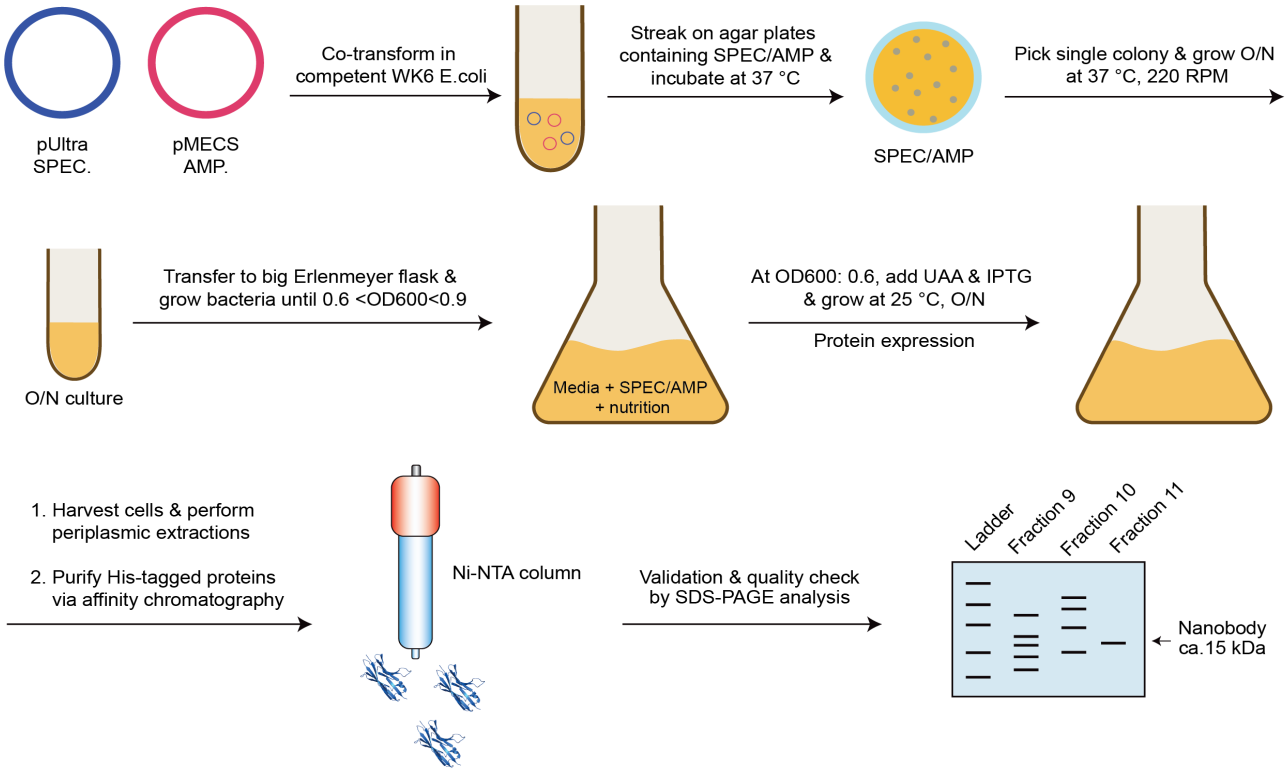

Figure 1. Bacterial expression of N- or C-terminal pAzF-nanobody. The competent WK6 *E. coli* strain is double-transformed with the plasmids pUltra and pMECS, the latter containing the nanobody sequence with either an N- or C-terminal amber stop codon (UAG), and are streaked on AMP/SPEC-containing agar plates and incubated O/N at 37°C. The following day a single colony is transferred to 2× TY supplemented with appropriate antibiotics to prepare an O/N culture. This pre-culture is transferred to a large Erlenmeyer flask containing TB medium, nutrition and antibiotics. Cells are grown at 37°C under shaking until OD600 ~0.6 at which point pAzF is added to the culture and induced with IPTG. Protein expression is performed at 25°C, shaking O/N. Once the cells are harvested, nanobodies are extracted from the periplasm prior to affinity chromatography purification on a Ni-NTA column. The purified nanobodies are analyzed by SDS-PAGE.

6. Thaw competent WK6 cells on ice for 30 min. Add 100 ng of each plasmid (pUltra and pMECS) to the cells and incubate on ice for another 30 min.
7. Heat shock the transformed cells by incubation at 42°C for 45 s and place the tubes on ice for 2 min.
8. Add 200 µl SOC media and incubate the cells at 37°C on shake 220 RPM for 0.5–1 h to allow for growth and maximal transformation efficiency (see Note 1).
9. Plate the cells on pre-warmed LB agar plates containing 100 µg/ml AMP and 100 µg/ml SPEC and incubate at 37°C O/N.
10. Transfer one discrete colony to 10 ml 2× TY containing 100 µg/ml AMP, 100 µg/ml SPEC and incubate at 37°C O/N at 220 RPM (see Note 2).
11. Transfer 5 ml O/N culture to 1 L TB medium in an Erlenmeyer flask supplemented with 100 ml salt buffer, 1 ml 2 M $MgCl_2$, 1 ml 50 mg/ml AMP, 1 ml 50 mg/ml SPEC and 10 ml 10% glucose solution. Monitor growth by measuring OD600 (see Note 3).

12. At 0.6 < OD600 < 0.9, add 1 ml 1M IPTG and pAzF (final concentration 1 mM or 0.202 g/L) to start the nanobody expression. Transfer the bacterial culture to 25°C and 200 RPM O/N corresponding to approx. 16 h (see Hints).

NOTES: (1) This step is crucial for selection of bacteria expressing antibiotic-resistant proteins to allow growth on antibiotic-containing agar plates. (2) For the best result, use a 100 ml conical flask for the O/N incubation. (3) Make sure to take out a blank sample for UV spectroscopy before adding the O/N culture.

HINTS: (1) Induction at different OD600 values ranging between 0.6–0.9 is a parameter that can be optimized for improved yields. (2) To increase nanobody yields upon induction, parameters that can be optimized are incubation time, temperature, and a higher RPM speed.

Purification of nanobodies by affinity chromatography

Nanobodies contain a stabilizing disulfide linkage and their folding therefore benefits from taking place in an oxidative environment such as the periplasm of *E. coli*, to ensure proper function and stability [22]. In our protocol, an N-terminal pelB leader signal sequence (MKYLLPTAAAGLLLLAAQPAMA) is used for translocation of pAzF-nanobodies to the periplasm. Extraction from the periplasm is done upon osmotic shock using EDTA-containing hyperosmotic TES buffer followed by cold hypotonic TES buffer [23]. The His-tagged nanobodies are purified by affinity chromatography using Ni-NTA resin, however other purification methods (size exclusion or ion-exchange chromatography) can also be employed. A description of pAzF-nanobody purification is found below. **Figure 2** shows a representative chromatogram of the elution profile and analysis of prominent peaks by SDS-PAGE gel.

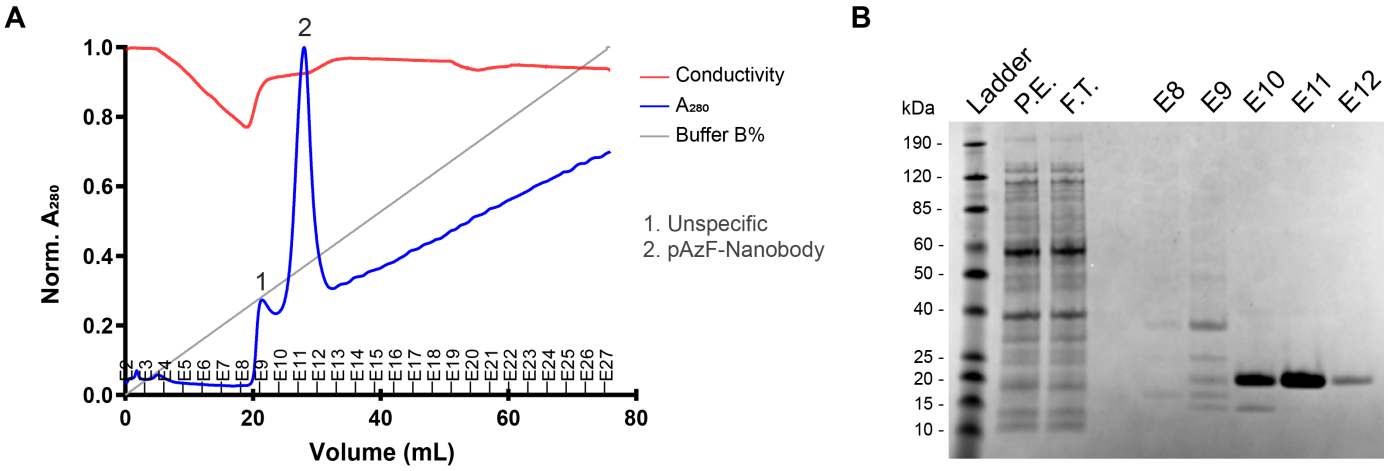

Figure 2. Purification of C-terminal pAzF-2Rb17c. A. A representative chromatogram showing the elution profile of His-tagged p-AzF-2Rb17c from affinity chromatography using a HisTrap column. **B.** Representative SDS-PAGE gel (4%–12%) showing from left: ladder, periplasmic extract (P.E.), flow through (F.T.), eluted fractions E8-12 for pAzF-2Rb17c from affinity chromatography purification.

13. Transfer culture to 1 L centrifuge flasks. Centrifuge for 30 min at 4°C and 4500 RPM.
14. Discard the supernatant and resuspend the pellet in 24 ml/L ice-cold TES solution. Transfer to 50 ml tubes and incubate at 4°C for 1 h and 200 RPM on a horizontal rotator (see Notes and Caution).
15. Add 48 ml 1:4 TES solution and incubate 1 h at 4°C, 200 RPM.
16. Centrifuge the cell suspension for 30 min at 4°C and 4500 RPM.
17. Decant the supernatant into 50 ml falcon tubes. This is the periplasmic extract; it can be stored in the freezer for up to 1 week. However, we recommend proceeding directly to the affinity chromatography step to avoid protein precipitation.
18. Add $MgCl_2$ to the periplasmic extracts to a final concentration of 1 mM. Centrifuge the samples at 9500× *g* to remove any residual cell remnants. Filter the entire sample through a 0.8 µm filter and subsequently through a 0.22 µm filter. Add imidazole to a final concentration of 10 mM (see Caution).

19. Prepare the ÄKTA Start system according to the manufacturer's guidelines. Make sure to flush any residual buffer from the system before attaching the column. Attach the 5 ml HisTrap column. Pre-run the column with binding buffer for at least 10 column volumes.
20. Begin loading the sample at flow rate 2 ml/min and increase to a flow rate 3–4 ml/min (see Notes and Caution).
21. When loading is complete, wash the column with at least 10 column volumes of binding buffer until the UV spectrum has reached baseline at approx. 10 mAu.
22. Elute samples by running a gradient of the binding buffer with elution buffer at a flow rate of 1 ml/min over 1 h.
23. Use the ÄKTA Start software, Unicorn, to analyze the elution profile. Collect prominent peaks and analyze them by SDS-PAGE and combine fraction samples with high protein concentrations. We usually combine 2–3 fractions in a total volume of 6–9 ml.
24. Transfer samples to a Slide-A-Lyzer Dialysis Cassette (3.5K MWCO cut-off) and dialyze O/N against 1× PBS (see Hints). Concentrate the nanobody using Amicon Ultra-4 Centrifugal Filter Units (3K MWCO cut-off) according to manufacturer's guidelines (see Hint). Determine nanobody concentration by measuring absorbance at 280 nm using a spectrophotometer, such as a DeNovix NanoDrop.

NOTES: (1) Make sure the cell pellet is completely resuspended before proceeding. Vigorous pipetting or the use of a vortex mixer can help to solubilize the pellet. (2) It is also recommended to collect the sample flow through in a separate glass bottle for subsequent gel analysis. In case the column was not well-equilibrated with binding buffer, the sample flow-through can be re-loaded onto the column for a new affinity chromatography run.

CAUTION: (1) Excessive vortexing could cause cell lysis and the release of histidine-rich proteins, which could compromise nanobody purity upon affinity chromatography purification. (2) The $MgCl_2$ is important as it binds to the EDTA present in the TES buffer. In the absence of Mg^{2+}, the EDTA may remove the Ni^{2+} from the HisTrap column. (3) It is important not to let any air enter the column, as it could compromise the His-tag binding to the resin. Do not load the entire periplasmic extract, but leave a volume of 100–500 µl.

HINT: It is possible to concentrate samples using Amicon Ultra-4 Centrifugal Filter Units (3K MWCO cut-off). Avoid concentrating samples above 1 mg/ml as this can cause protein aggregation or precipitation.

Site-specific bioconjugation reactions

DNA-PAINT super-resolution microscopy requires that a single-stranded (ss) DNA strand, also referred to as a docking strand, is attached to a binder in order to image a POI. Herein we used the concatenated DNA sequence 7× R3d (CTC TCT CTC TCT CTC TCT C), developed by Strauss and Jungmann for DNA-PAINT [24], however any DNA or RNA sequence can, in principle be used. For site-specific conjugation of a DNA oligonucleotide (19 nt) to the pAzF-nanobody, we employed the biorthogonal strain-promoted alkyne-azide cycloaddition (SPAAC) copper-free click chemistry [25] using a dibenzocyclooctyne (DBCO) at the 5′ end of the DNA strand (**Fig. 3A**). To establish the optimal conjugation ratios, reactions between the DBCO-modified oligonucleotide and pAzF-nanobody were carried out in 1:1, 1:2 or 1:4 ratios O/N at 700 RPM shaking at RT. The conjugation efficiency was assessed by denaturing urea PAGE and SDS-PAGE, which demonstrated a near complete reaction using between 1–2-fold excess of pAzF-nanobody (**Fig. 3B** and **3C**). Based on these data, we performed all subsequent conjugation reactions using a 2-fold excess of pAzF-nanobody as described below.

25. Mix 10 nmol of DBCO-labeled DNA oligonucleotide with 20 nmol of pAzF-modified nanobody in 1× PBS. For labeling with DBCO-modified fluorophore (DBCO-Cy5) use a 2-fold excess of the dye (see Hint).
26. Incubate reactions O/N (14–16 h) at 700 RPM shaking at RT. Keep reactions with fluorophores in the dark.
27. Evaluate reaction efficiencies by SDS-PAGE. For DNA-nanobody conjugates, a denaturing urea PAGE gel should also be performed in addition to SDS-PAGE gel prior to purification steps in order to visualize the DNA.

HINT: Reaction kinetics are improved by using high starting concentrations of DNA oligonucleotide (100–500 µM) and pAzF-nanobody (60–100 µM). Depending on the compound to be conjugated to the nanobodies, the yields can further be enhanced by incubation at 30–37°C.

Purification of bioconjugates using anion-exchange chromatography

We used anion-exchange chromatography to obtain highly pure DNA-nanobody bioconjugates, utilizing the

negative charge of the DNA. We observed that elution of the three different DNA-nanobody bioconjugates (5× R1d-2Rs15d, 7× R3d-2Rb17c and 7× R3d-VCAM1-5) occurs between 60% and 80% elution buffer B. **Figure 4A** shows a representative elution profile for purification of 7× R3d-2Rb17c. Each bioconjugate was resolved on a denaturing urea PAGE and SDS-PAGE indicating pure bioconjugates (**Fig. 4B** and **4C**).

pAzF-nanobodies conjugated to Cy5-DBCO were purified using desalting spin columns containing high-performance size-exclusion chromatography resin to remove excess Cy5-DBCO. This yielded pure Cy5-labeled pAzF-nanobodies, as visualized by SDS-PAGE (**Fig. 4D**). The purification steps for ion-exchange and size-exclusion chromatography are described in detail in the following section.

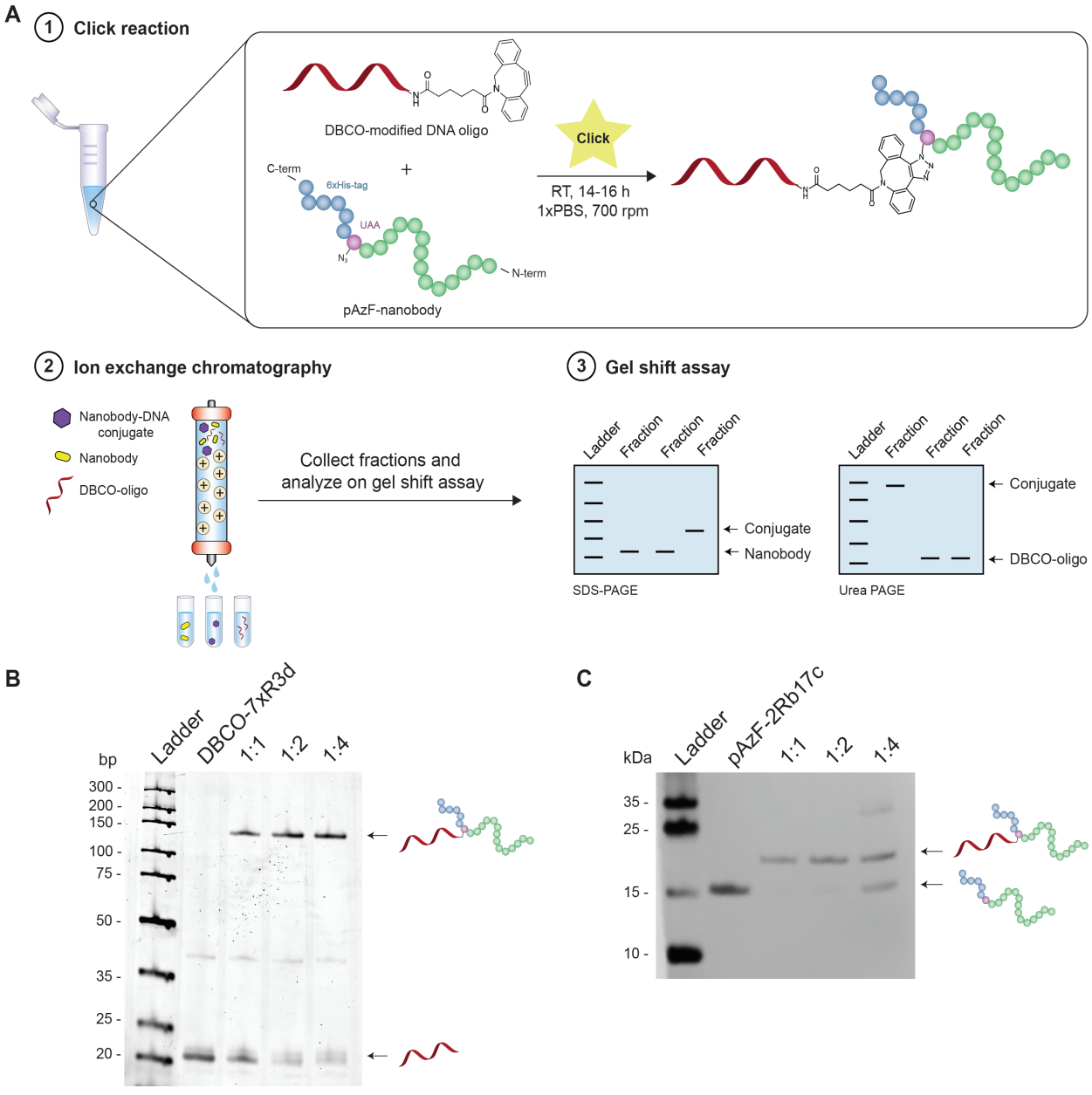

Figure 3. Optimization of bioconjugation reactions. A. Schematic illustration of the procedure for nanobody DNA oligonucleotide bioconjugation. The first step includes a SPAAC click reaction between pAzF nanobody and a DBCO-modified DNA oligonucleotide in a 2:1 ratio to form a stable triazole bond. The nanobody-DNA conjugates are subsequently purified using ion-exchange column to remove excess nanobody from the bioconjugate. Finally, the fractions containing the bioconjugate are analyzed for purity by gel shift assay on a SDS and Urea PAGE. **B.** 12% denaturing PAGE of conjugation efficiency between DBCO-modified DNA oligonucleotide and pAzF-Rb17c. Click reactions were conducted at the indicated pAzF-nanobody ratios. The gel was stained with SYBR Gold nucleic acid stain. The size marker is an ultra-low range DNA ladder (10–300 bp). **C.** SDS-PAGE gel showing the same reactions from (B) in a silver stain. The ladder is a PageRuler prestained protein ladder (10–180 kDa). Arrows indicate unreacted DBCO-modified DNA oligonucleotide (B) and pAzF-nanobody (C).

28. For purification of DNA-nanobody bioconjugates, prepare the anion exchange column by flushing the column with ion exchange binding buffer A (20 mM Tris, pH 8.0).

29. Dilute the bioconjugation reaction with ion exchange binding buffer to a total volume of 0.9 ml and inject it into the sample injection loop (see Notes).

30. Wash the column with 5 column volumes of ion exchange binding buffer. Elute the oligonucleotides using a linear gradient (0–100%) of ion-exchange elution buffer B (20 mM Tris pH 8.0, 500 mM NaCl). Unreacted nanobody will elute early, while the bioconjugates should elute before any unreacted oligonucleotides at ~90% elution buffer B (**Fig. 4A**). Therefore, avoid collecting samples of more than 0.5 ml.

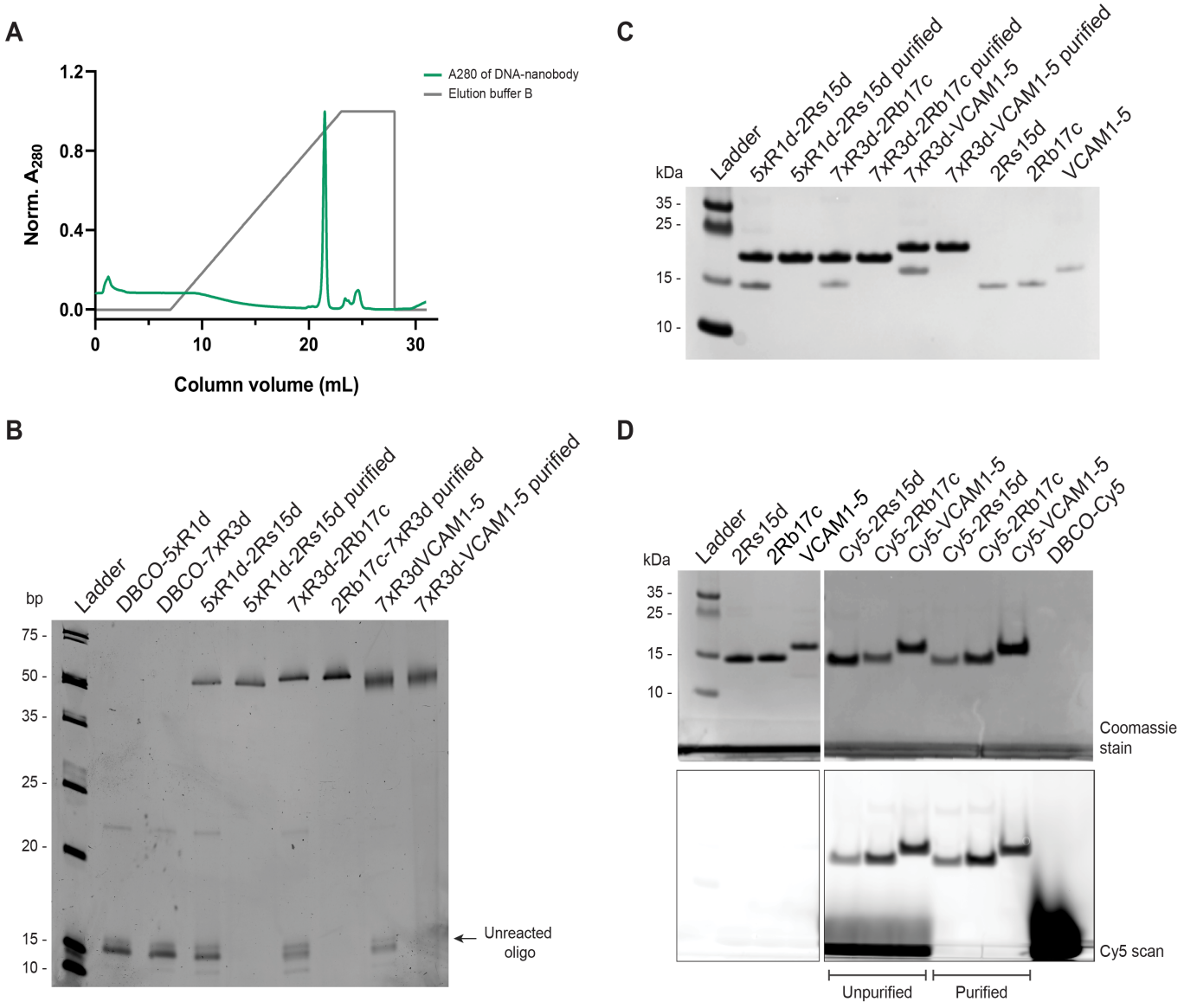

Figure 4. Site-specific labeling of C-terminal pAzF-nanobody with DNA oligonucleotide or Cy5 dye. A. Elution profile of DNA-nanobody bioconjugate purification using anion-exchange chromatography. **B.** 12% denaturing urea PAGE gel showing unlabeled DNA oligonucleotides or DNA-nanobody bioconjugates before or after purification. Gel is stained with SYBR gold nucleic acid stain and an ultra-low range size marker (10–300 bp) was used. **C.** SDS-PAGE gel indicating unpurified and purified DNA-nanobody bioconjugates. The gel is silver stained and the size marker is a PageRuler prestained protein ladder (10–180 kDa). **D.** SDS-PAGE gel visualizing unpurified and purified Cy5-labeled pAzF-nanobodies. The upper gels are stained with Coomassie brilliant blue and the lower gels are scanned for Cy5 signal.

31. Inspect the prominent peaks by denaturing urea PAGE and/or SDS-PAGE (**Fig. 4B** and **4C**).

32. Perform buffer-exchange with 1× PBS and concentrate the samples using Amicon Ultra-4 3K or 5K Centrifugal Filter Units (see Hints).

33. For Cy5-labeled nanobodies, excess Cy5-DBCO can be rapidly removed using Zeba Spin Desalting Columns (7K MWCO) by following manufacturer's instructions for "Buffer Exchange Procedure".

NOTE: We use a manual sample injection loop with a total volume of 1 ml. If a different setup is used, dilute the sample accordingly. Avoid injection of air into the system when using a manual sample injection loop.

HINT: The Amicon spin columns can also be used for buffer exchange. While concentrating the bioconjugates, simply add 1× PBS over three rounds of buffer exchange to assure complete removal of salt.

Validation of target binding of nanobody-oligonucleotide conjugates

We validated the integrity and target specificity of the nanobodies after bioconjugation by bio-layer interferometry (BLI) binding experiments.

Fc-HER2 or Fc-VCAM1 (2 µg/ml) were immobilized on a Protein A biosensor as recommended by the manufacturer (Sartorius). The bound receptors were subsequently probed with a titration of pAzF-nanobodies or DNA-nanobody bioconjugates starting from 100 nM to 1.5 nM (2Rb17c and 2Rs15d) or 50 nM to 0.7 nM (VCAM1-5). To investigate whether the introduction of a DNA strand to either the C- or N-terminal ends of the two HER2 nanobodies can obstruct their binding to the HER2 receptor, both C- and N-terminal pAzF-2Rb17c- and -2Rs15d were included in the binding assay.

BLI binding experiments of pAzF-nanobodies and the bioconjugates were conducted on an OctetRED96e system as described below and results are shown in **Figure 5**.

34. Prehydrate the Protein A biosensors in binding buffer (1× PBS, 0.02% Tween-20, 0.05% BSA) for 15 min at RT.
35. Dilute the protein target (Fc-HER2 or Fc-VCAM1) to 2 µg/ml in binding buffer and transfer 200 µl to a column in a 96-well flat-bottom black plate.
36. In the 96-well plate, prepare a 2-fold serial dilution of the nanobodies or nanobody bioconjugates in binding buffer starting with the highest concentration. Leave one well as reference well containing only binding buffer.
37. Set up the Octet software according to the manufacturer's guidelines for Kinetic Analysis, adjust the parameters for association and dissociation time scales and start data acquisition.
38. Analyze the binding profile in the Octet Data Analysis software and fit data to a 1:1 Binding model to obtain rate constants and K_D values.

Application of nanobody-oligonucleotide bioconjugates for DNA-PAINT

We performed DNA-PAINT using the HER2-specific nanobody 2Rs15d to demonstrate the applicability of the site-specifically labeled DNA-nanobody bioconjugates for super-resolution microscopy.

The experimental details for sample preparation and imaging with DNA-PAINT on HER2-positive cells are presented below.

Sample preparation

39. One day prior to DNA-PAINT imaging, seed SkBr3 and SKOV3 cells in an Ibidi 8-well glass-bottom µ-Slide as 30000 and 20000 cells per well, respectively.
40. The following day, rinse cells with 1× PBS twice and fix with 300 µl 37°C pre-heated 4% paraformaldehyde solution for 15 min at RT followed by three wash steps of 5 min using 1× PBS.
41. Permeabilize cells with 300 µl 0.2% Triton-X100 solution for 10 min at RT.
42. Block the cells with 300 µl blocking buffer (1× PBS, 3% BSA, 1 mM EDTA, and 0.02% Tween-20) at RT in the dark for 1.5 h.
43. Dilute the 5× R1d-2Rs15d nanobody-DNA bioconjugate in blocking buffer supplemented with 0.05 mg/ml salmon sperm DNA to block for unspecific binding from the DNA strand. Stain the cells with 20 nM of the bioconjugate at RT in the dark for 1 h (see Notes).
44. Wash the cells three times of 5 min.
45. Prepare a 1:3 dilution of 90 nm gold nanoparticles in buffer C (1× PBS, 500 mM NaCl, 1 mM EDTA). Add 300 µl to the cells and incubate for 5 min, subsequently wash the cells three times to remove excess gold nanoparticles.

46. Prepare imager solution comprising buffer C supplemented with the PCA/PCD oxygen scavenging system [26]: to 1 ml imager solution, mix 955 µl buffer C with 25 µl PCA (40×), 10 µl Trolox (100×) and 10 µl PCD (100×) and finally add 1 µl 3′-end Cy3B-labeled R1i/7nt imager strand to a final concentration of 1 nM.

NOTE: Cells can also be stained at 4 °C in the dark O/N (14–16 h).

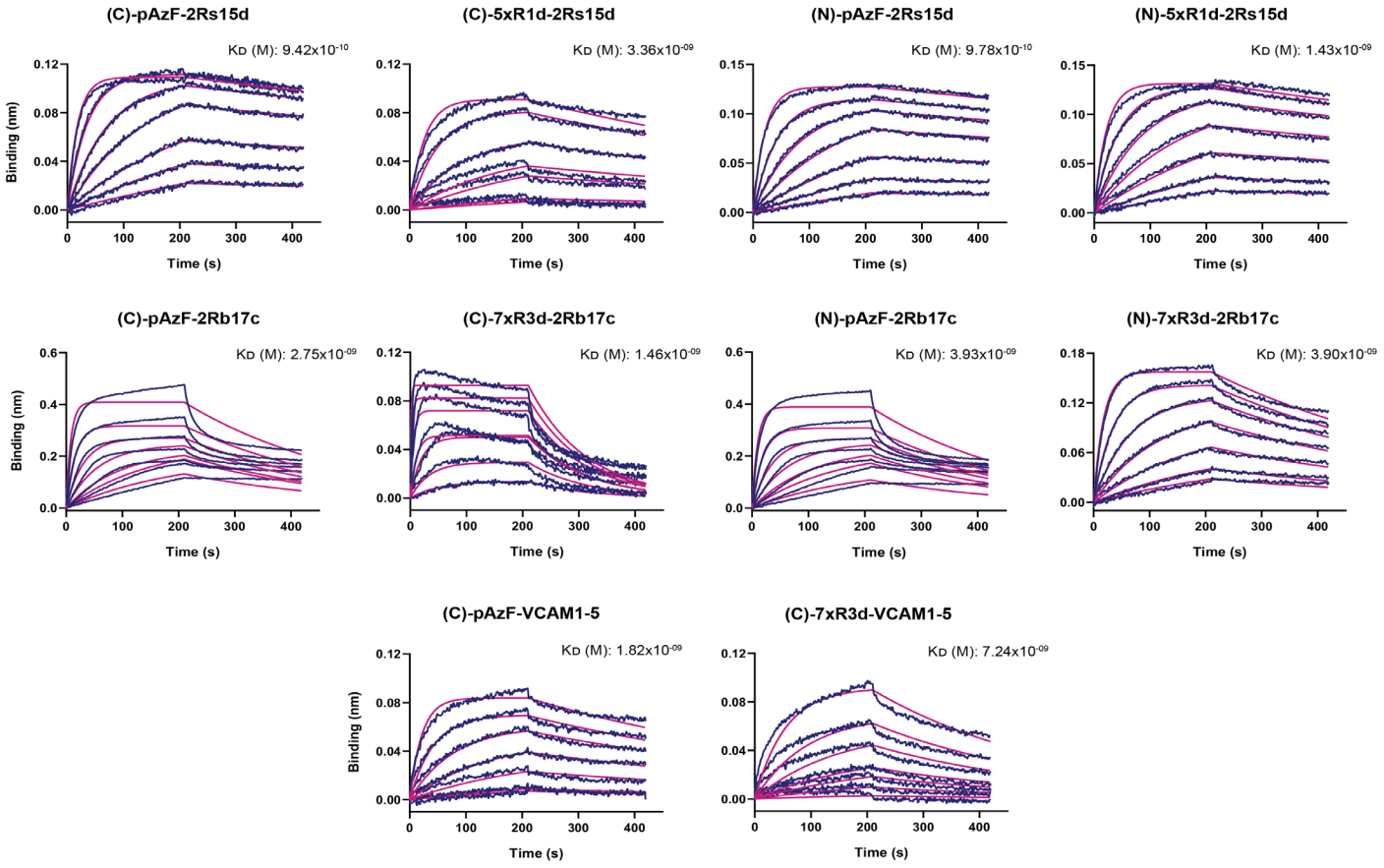

Figure 5. Binding profile of pAzF-modified nanobodies and DNA-nanobody bioconjugates. Bio-layer interferometry (BLI) sensograms illustrating the binding profiles of pAzF-modified nanobodies and their corresponding conjugates. Kinetic analysis was performed on the raw binding data (dark blue color) by fitting to a 1:1 binding model (pink) to extract association and dissociation rate constants, as well as the equilibrium dissociation constant K_D given in Molar (M) for each nanobody and bioconjugate. Top panel: C- or N-terminal pAzF-2Rs15d nanobody or DNA-modified bioconjugates (5× R1d-2Rs15d) interacting with human HER2 receptor. Middle panel: C- or N-terminal pAzF-Rb17c nanobody or DNA-modified bioconjugates (7× R3d-2Rb17c) binding to human HER2 receptor. Bottom panel: C-terminal pAzF-VCAM1-5 nanobody and the bioconjugate 7× R3d-VCAM1-5 binding to murine VCAM1 receptor. HER2- and VCAM1-5-specific nanobodies and their corresponding conjugates were titrated in a 2-fold serial dilution in the concentrations 100 to 1.5 nM and 50 to 0.7 nM, respectively.

Microscope setup and image analysis

DNA-PAINT fluorescence imaging was conducted on an inverted microscope (Oxford Nanoimager S) with an in-built real-time autofocus system and an objective (100×, oil immersion, NA 1.4) configured to total internal reflection fluorescence microscopy (TIRFM). For excitation of the Cy3B dye the 561 nm laser line was used with a power density of 25 W/mm^2. The images were acquired on a sCMOS camera with pixel size of 117 nm using an exposure time of 100 ms and collecting 30000 and 40000 frames for SkBr3 and SKOV3 cells, respectively.

For the reconstruction of a super-resolved image, as seen in **Figure 6**, raw fluorescence data was processed using a modified version of the Picasso software package [27] adapted to Gigabit-size TIFF files. In Picasso:Localize, individual spots were localized and fitted to the Maximum Likelihood Estimation (MLE) followed by rendering of a super-resolution image in Picasso:Render. The images were drift-corrected by redundant cross-correlation and subsequently by picking several gold nanoparticles as fiducial markers. Lastly, localizations with spot widths that were too large or too small were filtered out in Picasso:Filter.

ANTICIPATED RESULTS & TROUBLESHOOTING

The method presented herein allows for bioorthogonal SPAAC conjugation of oligonucleotides or fluorescent dyes to recombinant nanobodies carrying a UAA inserted site-specifically at either the N- or C-terminus. Our nanobody expression in bacteria generally results in protein yields between 0.6 and 1 mg/L of culture, that can be visualized as distinct bands on an SDS-PAGE gel. However, the expression yields for each nanobody can be sequence-dependent and the proposed expression conditions may need to be optimized further for the individual protein. The reactivity of the resulting azide-functionalized nanobody should be high and result in > 95% reacted bioconjugates when performed with an excess of nanobody to oligonucleotide. Following conjugation and purification, the target-binding abilities should be preserved and the affinity of the nanobody must be equivalent to an unconjugated nanobody in a binding assay such as BLI.

Possible problems during the procedures and their solutions are provided in **Table 1**.

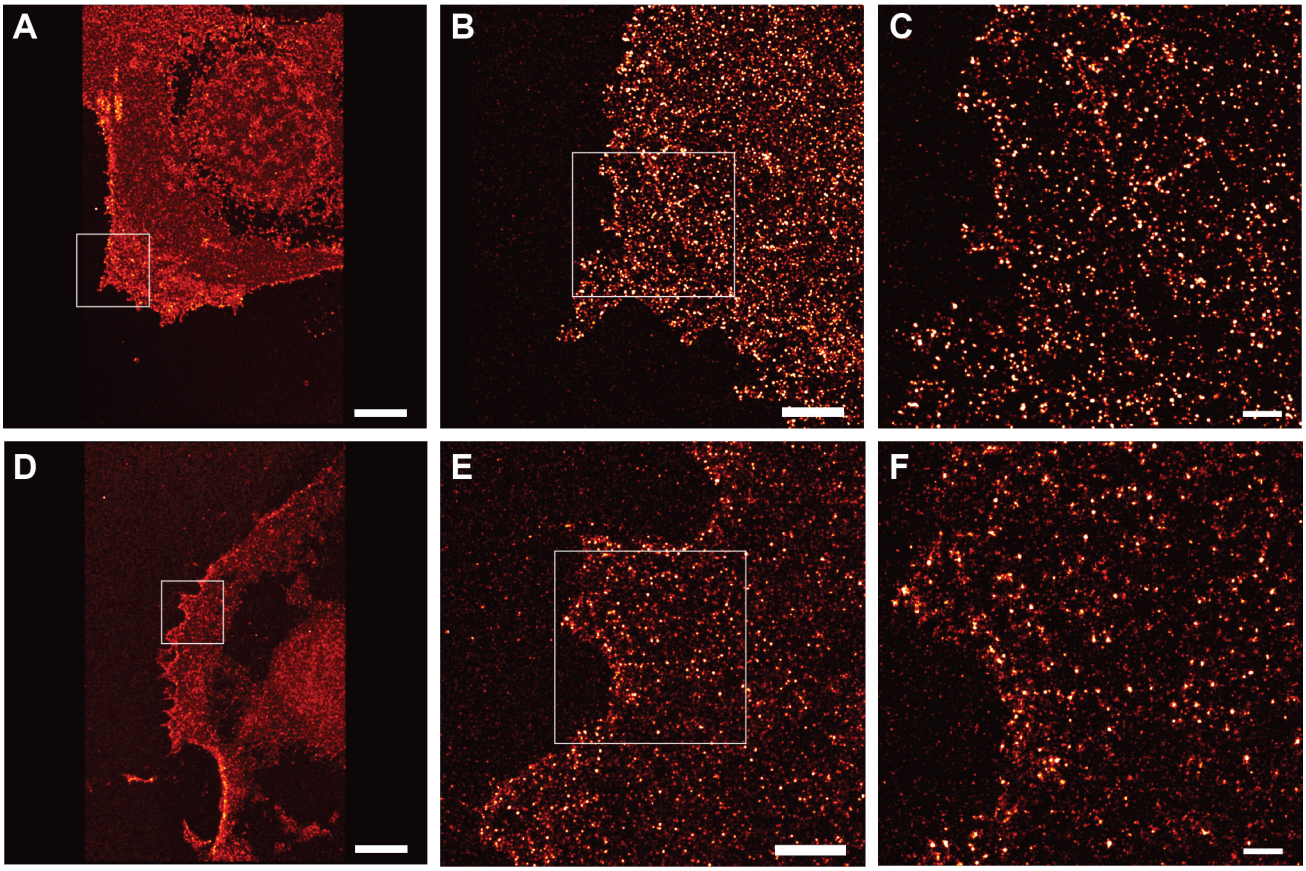

Figure 6. DNA-PAINT of anti-HER2-nanobody bioconjugate. Reconstructed DNA-PAINT images of a representative SkBr3 (A-C) or SKOV3 cell (D-F) stained with 5× R1d-2RS15d bioconjugate (20 nM). **B-C.** Close-up view of the outlined areas (white box) in (A) and (B) showing a high cell surface density of the HER2 receptor as indicated by the individual bright spots. **E-F.** Close-up view of the indicated boxes in (D) and (E) presents a lower HER2 receptor density. Localization precision is given as nearest neighbor based analysis (NeNA), which is approximately 4 nm for both SkBr3 and SKOV3 cells. Scale bar: 10 μm (A, D), 2 μm (B, E), 500 nm (C, E).

DISCUSSION

In this study, we have expressed nanobodies containing the pAzF at either the N- or C-terminus. The UAA can be inserted at any desired site in the nanobody sequence [17]. However, an internal position may require some optimization, preferentially with knowledge from the crystal structure of the nanobody-receptor complex, to avoid reduced antigen binding. The anti-HER2 nanobodies, 2Rs15d and 2Rb17c, were expressed and purified with the pAzF modification on either the N- or C-terminus, while VCAM1-5 was expressed only with C-terminal pAzF. High yields (> 0.6 mg/L) were obtained for VCAM1-5 and 2Rb17c regardless of the location of pAzF. Both N- or C-terminal pAzF-2Rs15d gave relatively low yields of ~200 μg/L and < 100 μg/L, respectively.

We believe the lower yields associated with the pAzF-2Rs15d nanobody may be due to the high number of cysteine residues in the protein sequence [28] that are essential for the stability of the tertiary structure of the nanobody. Formation of disulfide bonds with incorrect cysteine pairs can influence protein folding and stability and may therefore make the nanobody subject to proteolytic degradation or result in the unproductive formation of inclusion bodies [28,29].

For the bioconjugation reactions, the amount of oligonucleotide will often be the limiting factor as this is often purchased or provided by an external lab, while the nanobody can be produced in-house in high amounts as shown here. We therefore investigated the ideal ratio

of oligonucleotide and nanobodies in the click reactions, keeping the nanobody in excess. We found that a 2-fold excess of protein led to a high conversion rate and that increasing the ratio to 1:4 (oligonucleotide:nanobody) did not increase the reaction yields. Performing the reactions in a 1:2 ratio will ensure a lower waste of materials than if a larger excess of nanobody is used but does require somewhat precise quantification of the protein after purification.

We purified the oligonucleotide-nanobody conjugates by anion-exchange chromatography. The DNA oligonucleotide is the main contributor to electrostatic interactions with the positively charged column matrix. However, the pI of different nanobodies can have an impact on the elution profile. We therefore recommend that a smaller sample is purified first, and that all fractions from the relevant peaks are collected and analyzed on a gel to localize the desired product, before the bulk bioconjugate sample is purified.

In order to confirm that the nanobodies in the bioconjugates had retained their function, we performed a series of BLI binding experiments using recombinant murine Fc-VCAM1 or human Fc-HER2 receptor as targets. Other similar techniques, like surface plasmon resonance (SPR) using BIACORE instruments can also be used.

For the HER2-specific nanobodies, there was only negligible difference in apparent K_D between the pAzF-modified 2Rb17c nanobody and the corresponding DNA-conjugated nanobody (**Fig. 5**, middle panel). On the contrary, we observed an increase in K_D (lower binding efficiency) by nearly one order of magnitude for DNA-conjugated 2Rs15d nanobody compared to free nanobody (**Fig. 5**, upper panel). Nonetheless, the binding affinity of both HER2-specific nanobody conjugates remained in the low nanomolar range, which is in accordance with the K_D values for the unconjugated nanobodies reported by Vaneycken *et al*. [19]. Furthermore, the introduction of a DNA oligonucleotide to either the C- or N-terminus of 2Rb17c and 2Rs15d did not obstruct the binding to their cognate receptor as observed from the low K_D values (**Fig. 5**, top two panels). In some cases, N-terminal modifications of nanobodies can impair antigen-binding since the CDR loops are positioned adjacent to this site (**Fig. 7**). It is therefore more common to introduce alterations to the more distant C-terminus. However, this is nanobody sequence-dependent and may require further optimization prior to large-scale production.

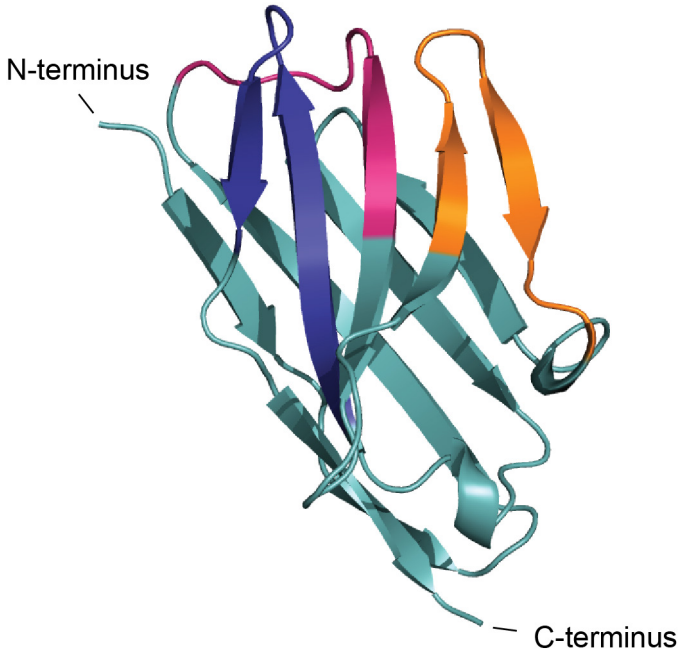

Figure 7. Nanobody CDRs. Crystal structure of 2Rs15d nanobody. The three indicated CDR loops (pink, orange and purple represent CDR1, CDR2 and CDR3, respectively) are oriented towards the N-terminus side. The figure was created in Pymol using the PDB entry (ID 5MY6).

Similar to the 2Rs15d conjugate, the binding affinity of the VCAM1-5-specific nanobody conjugate was only slightly compromised (**Fig. 5** bottom panel), as the apparent K_D value remained below 10 nM compared to that recorded for the azido-modified and published nanobody (K_D ~2 nM) [19].

DNA-PAINT is an SMLM technique that relies on the transient binding of a short fluorophore-labeled DNA strand to its complementary docking strand coupled to a ligand binding the POI [27]. Thousands of frames of stochastic blinking in a TIRF configuration [30,31] are acquired in order to computationally reconstruct a super-resolution image. We chose HER2 as a target for DNA-PAINT microscopy since expression of this cell surface receptor is upregulated in a breast cancer subtype associated with medium-to-high death rates, and it is therefore a biomarker of great interest for both biomedical research and clinical imaging [32]. The previously reported HER2-specific 2Rs15d nanobody displays a slow dissociation rate constant (5.71×10^{-4} s^{-1}) making it an ideal binder for super-resolution microscopy [18]. For this reason, we used pAzF-2Rs15d nanobody conjugated to DBCO-modified docking DNA speed sequence 5× R1d [24] on HER2 positive breast and ovarian cancer cell lines, SkBr3 and SKOV3, respectively.

The SKOV3 cell line is known to have a medium HER2 expression level compared to other breast cancer cell lines [33]. This is in accordance with the observed density of single molecules seen in our DNA-PAINT analysis (**Fig. 6**, lower panel), representing individual HER2 receptors

on the cell surface. In contrast, HER2 expression is substantially upregulated in SkBr3 cells, which correlates with the higher density of HER2 molecules shown in **Figure 6**, upper panel. The achieved localization precisions calculated by nearest neighbor based analysis (NeNA) were ~4 nm for both SkBr3 and SKOV3 images.

The expression and labeling strategy shown here enables site-specific, stoichiometric nanobody modification and yields a homogeneous sample. The nanobodies are efficiently produced in bacteria in reasonable amounts, and the reactivity of the azide functional group as well as the nanobody affinity and target-binding ability are preserved. Owing to its simplicity and versatility, this method can be easily adapted to research laboratory-scale, on-demand production of modified nanobodies, offering customized labeling for direct use in targeting assays. As site-specificity and stoichiometric control is essential for generating super-resolved microscopy images, the present protocol therefore shows a method for producing high-affinity nanobody conjugates as highly specific imaging agents for use in techniques such as DNA-PAINT microscopy. However, a number of other applications within areas such as targeted drug delivery, can benefit from site-specific conjugation of nanobodies to oligonucleotides like siRNAs [34] or drug delivery scaffolds [35]. We believe that the present protocol is highly flexible and could readily be adapted for use with any biologically interesting nanobody or nucleic acid.

Table 1. Troubleshooting.

Step	Problems	Causes	Suggestions
11	Slow and/or poor bacterial growth	• Poor flask oxygenation • Inoculation of low-density O/N culture • Dense foam disrupting culture aeration • Excess of antifoam agent disrupting aeration	• Use Erlenmeyer flasks with baffles • Increase RPM speed • Prolong O/N culture up to 14 h • Use antifoam agents • Reduce the use of antifoam agent [36,37]
12	Poor nanobody yield	Expression conditions such as O/N culture incubation, OD600 used for the induction or UAA concentration need to be optimized	Perform 250 ml test cultures applying different conditions to select the best strategy for higher scale nanobody production
24	Decreased nanobody reactivity over time	Improper nanobody storage	For short-term use, store nanobodies in 50% glycerol at −20°C. For long-term storage, store working-size aliquots of the nanobody solution at −80°C

Acknowledgments

The authors thank the past and present members of the Kjems lab for their contribution to this work. We are grateful to Ralf Jungmann and Alexandra Eklund for their invaluable advice on DNA-PAINT. A big thanks to the Center Manager for Cellular Signal Patterns (CellPAT) Anne F. Nielsen for reading and editing this manuscript. This work was supported by grant DNRF135 from the Danish National Research Foundation to the Center for Cellular Signal Patterns (CellPAT) and, in part, by the Novo Nordisk Foundation to the Center for Multifunction Biomolecular Drug Design (CEMBID) (grant NNF17OC0028070).

References

1. Kijanka M, Dorresteijn B, Oliveira S, van Bergen en Henegouwen PM. Nanobody-based cancer therapy of solid tumors. Nanomedicine (Lond). 2015 Jan;10(1):161–74. https://doi.org/10.2217/nnm.14.178 PMID:25597775
2. Chakravarty R, Goel S, Cai W. Nanobody: the "magic bullet" for molecular imaging? Theranostics. 2014 Jan;4(4):386–98. https://doi.org/10.7150/thno.8006 PMID:24578722
3. Muyldermans S. Nanobodies: natural single-domain antibodies. Annu Rev Biochem. 2013;82(1):775–97. https://doi.org/10.1146/annurev-biochem-063011-092449 PMID:23495938
4. Lelek M, Gyparaki MT, Beliu G, Schueder F, Griffié J, Manley S, et al. Single-molecule localization microscopy. Nature Reviews Methods Primers. 2021;1(1):39. https://doi.org/10.1038/s43586-021-00038-x.
5. Betzig E, Patterson GH, Sougrat R, Lindwasser OW, Olenych S, Bonifacino JS, et al. Imaging intracellular fluorescent proteins at nanometer resolution. Science. 2006 Sep;313(5793):1642–5. https://doi.org/10.1126/science.1127344 PMID:16902090
6. Hess ST, Girirajan TP, Mason MD. Ultra-high resolution imaging by fluorescence photoactivation localization microscopy. Biophys J. 2006 Dec;91(11):4258–72. https://doi.org/10.1529/biophysj.106.091116 PMID:16980368
7. Rust MJ, Bates M, Zhuang X. Sub-diffraction-limit imaging by stochastic optical reconstruction microscopy (STORM). Nat Methods. 2006 Oct;3(10):793–5. https://doi.org/10.1038/nmeth929 PMID:16896339
8. Heilemann M, van de Linde S, Schüttpelz M, Kasper R, Seefeldt B, Mukherjee A, et al. Subdiffraction-resolution fluorescence imaging with conventional fluorescent probes. Angew Chem Int Ed Engl. 2008;47(33):6172–6. https://doi.org/10.1002/anie.200802376 PMID:18646237
9. Jungmann R, Steinhauer C, Scheible M, Kuzyk A, Tinnefeld P, Simmel FC. Single-molecule kinetics and super-resolution microscopy by fluorescence imaging of transient binding on DNA origami. Nano Lett. 2010 Nov;10(11):4756–61. https://doi.org/10.1021/nl103427w PMID:20957983
10. Pleiner T, Bates M, Trakhanov S, Lee C-T, Schliep JE, Chug H, et al. Nanobodies: site-specific labeling for super-resolution imaging, rapid epitope-mapping and native protein complex isolation. elife. 2015;4:e11349.
11. Ries J, Kaplan C, Platonova E, Eghlidi H, Ewers H. A simple, versatile method for GFP-based super-resolution microscopy via nanobodies. Nat Methods. 2012 Jun;9(6):582–4. https://doi.org/10.1038/nmeth.1991 PMID:22543348
12. Agasti SS, Wang Y, Schueder F, Sukumar A, Jungmann R, Yin P. DNA-barcoded labeling probes for highly multiplexed Exchange-PAINT imaging. Chem Sci (Camb). 2017 Apr;8(4):3080–91. https://doi.org/10.1039/C6SC05420J PMID:28451377
13. Sograte-Idrissi S, Schlichthaerle T, Duque-Afonso CJ, Alevra M, Strauss S, Moser T, et al. Circumvention of common labelling artefacts using secondary nanobodies. Nanoscale. 2020 May;12(18):10226–39. https://doi.org/10.1039/D0NR00227E PMID:32356544

14. Schlichthaerle T, Strauss MT, Schueder F, Auer A, Nijmeijer B, Kueblbeck M, et al. Direct visualization of single nuclear pore complex proteins using genetically-encoded probes for DNA-PAINT. Angew Chem Int Ed Engl. 2019 Sep;58(37):13004–8. https://doi.org/10.1002/anie.201905685 PMID:31314157
15. Massa S, Xavier C, De Vos J, Caveliers V, Lahoutte T, Muyldermans S, et al. Site-specific labeling of cysteine-tagged camelid single-domain antibody-fragments for use in molecular imaging. Bioconjug Chem. 2014 May;25(5):979–88. https://doi.org/10.1021/bc500111t PMID:24815083
16. Fabricius V, Lefèbre J, Geertsema H, Marino SF, Ewers H. Rapid and efficient C-terminal labeling of nanobodies for DNA-PAINT. J Phys D Appl Phys. 2018;51(47):474005. https://doi.org/10.1088/1361-6463/aae0e2.
17. Chatterjee A, Sun SB, Furman JL, Xiao H, Schultz PG. A versatile platform for single- and multiple-unnatural amino acid mutagenesis in Escherichia coli. Biochemistry. 2013 Mar;52(10):1828–37. https://doi.org/10.1021/bi4000244 PMID:23379331
18. Vaneycken I, Devoogdt N, Van Gassen N, Vincke C, Xavier C, Wernery U, et al. Preclinical screening of anti-HER2 nanobodies for molecular imaging of breast cancer. FASEB J. 2011 Jul;25(7):2433–46. https://doi.org/10.1096/fj.10-180331 PMID:21478264
19. Broisat A, Hernot S, Toczek J, De Vos J, Riou LM, Martin S, et al. Nanobodies targeting mouse/human VCAM1 for the nuclear imaging of atherosclerotic lesions. Circ Res. 2012 Mar;110(7):927–37. https://doi.org/10.1161/CIRCRESAHA.112.265140 PMID:22461363
20. Jungmann R, Avendaño MS, Dai M, Woehrstein JB, Agasti SS, Feiger Z, et al. Quantitative super-resolution imaging with qPAINT. Nat Methods. 2016 May;13(5):439–42. https://doi.org/10.1038/nmeth.3804 PMID:27018580
21. Richardson MB, Brown DB, Vasquez CA, Ziller JW, Johnston KM, Weiss GA. Synthesis and Explosion Hazards of 4-Azido-l-phenylalanine. J Org Chem. 2018 Apr;83(8):4525–36. https://doi.org/10.1021/acs.joc.8b00270 PMID:29577718
22. de Marco A. Recombinant expression of nanobodies and nanobody-derived immunoreagents. Protein Expr Purif. 2020 Aug;172:105645. https://doi.org/10.1016/j.pep.2020.105645 PMID:32289357
23. Nossal NG, Heppel LA. The release of enzymes by osmotic shock from Escherichia coli in exponential phase. J Biol Chem. 1966 Jul;241(13):3055–62. https://doi.org/10.1016/S0021-9258(18)96497-5 PMID:4287907
24. Strauss S, Jungmann R. Up to 100-fold speed-up and multiplexing in optimized DNA-PAINT. Nat Methods. 2020 Aug;17(8):789–91. https://doi.org/10.1038/s41592-020-0869-x PMID:32601424
25. Agard NJ, Prescher JA, Bertozzi CR. A strain-promoted [3 + 2] azide-alkyne cycloaddition for covalent modification of biomolecules in living systems. J Am Chem Soc. 2004 Nov;126(46):15046–7. https://doi.org/10.1021/ja044996f PMID:15547999
26. Aitken CE, Marshall RA, Puglisi JD. An oxygen scavenging system for improvement of dye stability in single-molecule fluorescence experiments. Biophys J. 2008 Mar;94(5):1826–35. https://doi.org/10.1529/biophysj.107.117689 PMID:17921203
27. Schnitzbauer J, Strauss MT, Schlichthaerle T, Schueder F, Jungmann R. Super-resolution microscopy with DNA-PAINT. Nat Protoc. 2017 Jun;12(6):1198–228. https://doi.org/10.1038/nprot.2017.024 PMID:28518172
28. de Marco A. Strategies for successful recombinant expression of disulfide bond-dependent proteins in Escherichia coli. Microb Cell Fact. 2009 May;8(1):26. https://doi.org/10.1186/1475-2859-8-26 PMID:19442264
29. Georgiou G, Valax P. Expression of correctly folded proteins in Escherichia coli. Curr Opin Biotechnol. 1996 Apr;7(2):190–7. https://doi.org/10.1016/S0958-1669(96)80012-7 PMID:8791338
30. Funatsu T, Harada Y, Tokunaga M, Saito K, Yanagida T. Imaging of single fluorescent molecules and individual ATP turnovers by single myosin molecules in aqueous solution. Nature. 1995 Apr;374(6522):555–9. https://doi.org/10.1038/374555a0 PMID:7700383
31. Tokunaga M, Kitamura K, Saito K, Iwane AH, Yanagida T. Single molecule imaging of fluorophores and enzymatic reactions achieved by objective-type total internal reflection fluorescence microscopy. Biochem Biophys Res Commun. 1997 Jun;235(1):47–53. https://doi.org/10.1006/bbrc.1997.6732 PMID:9196033
32. Harbeck N, Penault-Llorca F, Cortes J, Gnant M, Houssami N, Poortmans P, et al. Breast cancer. Nat Rev Dis Primers. 2019 Sep;5(1):66. https://doi.org/10.1038/s41572-019-0111-2 PMID:31548545
33. Gall VA, Philips AV, Qiao N, Clise-Dwyer K, Perakis AA, Zhang M, et al. Trastuzumab Increases HER2 Uptake and Cross-Presentation by Dendritic Cells. Cancer Res. 2017 Oct;77(19):5374–83. https://doi.org/10.1158/0008-5472.CAN-16-2774 PMID:28819024
34. Zavoiura O, Brunner B, Casteels P, Zimmermann L, Ozog M, Boutton C, et al. Nanobody-siRNA Conjugates for Targeted Delivery of siRNA to Cancer Cells. Mol Pharm. 2021 Mar;18(3):1048–60. https://doi.org/10.1021/acs.molpharmaceut.0c01001 PMID:33444501
35. Andersen VL, Vinther M, Kumar R, Ries A, Wengel J, Nielsen JS, et al. A self-assembled, modular nucleic acid-based nanoscaffold for multivalent theranostic medicine. Theranostics. 2019 Apr;9(9):2662–77. https://doi.org/10.7150/thno.32060 PMID:31131060
36. Koch V, Rüffer HM, Schügerl K, InSnertsberger E, Menzel H, Weis J. Effect of antifoam agents on the medium and microbial cell properties and process performance in small and large reactors. Process Biochem. 1995;30(5):435–46. https://doi.org/10.1016/0032-9592(94)00029-8.
37. Holmes W, Smith R, Bill R. Evaluation of antifoams in the expression of a recombinant FC fusion protein in shake flask cultures of Saccharomyces cerevisiae & Pichia pastoris. Microb Cell Fact. 2006;5(1):1–3.